

Would Diamond Nanorods Be Stronger than Fullerene Nanotubes?

Olga Shenderova,^{†‡} Donald Brenner,^{*†} and Rodney S. Ruoff[§]

International Technology Center, Research Triangle Park, North Carolina 27709, Department of Materials Science and Engineering, North Carolina State University, Raleigh, North Carolina 27695-7907, and Department of Mechanical Engineering, Northwestern University, Evanston, Illinois 60208

Received December 17, 2002; Revised Manuscript Received February 14, 2003

ABSTRACT

On the basis of literature *ab initio* data, we show that diamond nanorods would have a brittle fracture force and a zero strain stiffness that exceeds carbon nanotubes for radii greater than about 1–3 nm, depending on the orientation of the diamond nanorod. The energetic stability of diamond nanorods is predicted by molecular modeling to be comparable to single-walled carbon nanotubes. It is concluded that diamond nanorods represent an important and viable target structure for synthesis.

With its exceedingly high bulk modulus and hardness, diamond has historically been considered the strongest material. Recently, however, it has been claimed based on both theory and experiment that carbon nanotubes are both stiffer and stronger along their axis than diamond. A problem with this claim is that it is difficult to make a fair comparison between these two representatives from the macro- and nanoscales unless some additional assumptions about their structure are made, for example an effective “thickness” of a sheet of carbon atoms comprising a nanotube.

In this paper the mechanical properties of single-walled nanotubes (SWNTs) and multiwalled nanotubes (MWNTs) are compared to the predicted properties of an equivalent nanoscopic-scale diamond structure, namely a diamond nanorod (DNR). Our general analysis suggests that while a SWNT will have a higher strength-to-weight ratio, above a critical radius between about 1 and 3 nm (depending on the DNR structure) the force needed for brittle fracture of a DNR exceeds that of a SWNT. This higher fracture force, which at the nanoscopic scale is a less ambiguous property than fracture stress, results from the larger load-bearing cross-sectional area of DNRs compared to SWNTs at the same diameter. Similarly, the calculations show that the zero strain stiffness of DNRs will exceed that of SWNTs for radii greater than about 1 nm.

Experimental loading of SWNTs in ropes has yielded estimates for the tensile Young's modulus that range from 320 GPa to 1.47 TPa,¹ and breaking strengths that range from 13 to 52 GPa (a strain of up to almost 6%),¹ values that

Table 1: Selected Measured and Predicted Mechanical Properties of Bulk Diamond along Different Orientations, Graphite, and Graphene (related strains in parentheses)

structure	orientation	Young's modulus (GPa)	<i>ab initio</i> tensile strength (GPa)
diamond	⟨001⟩	1052 ^a	225 ^b ($\epsilon = 0.37$)
	⟨011⟩	1169 ^a	130 ^b ($\epsilon = 0.24$)
	⟨111⟩	1214 ^a	90 ^b ($\epsilon = 0.14$), 95 ^c ($\epsilon = 0.13$)
graphite		1020 ^d	
graphene	armchair		77 ^e nN/nm
	zigzag		71 ^e nN/nm

^a Calculated using experimental C_{ij} from ref 7. ^b Theoretical value from ref 9. ^c Theoretical value from ref 8. ^d From ref 27. ^e First principles estimate (ref 4).

agree well with theoretical estimates of yield strain.² Properties of SWNTs predicted from first principles calculations include a Young's modulus approaching that of a graphene sheet (~ 1.03 TPa³) and a fracture strength of ~ 200 GPa (Tables 1 and 2),⁴ assuming a 0.34 nm nanotube wall thickness. The failure strength estimated from theory and experiment for a SWNT is over a factor of 3 larger than established yield strengths for the strongest fibers typically used in fiber-reinforced composites (e.g., graphite, silicon nitride, silicon carbide, or aluminum oxide), which has made nanotubes attractive structures for reinforcing nanocomposites. More recently, the first observation using transmission electron microscopy of a MWNT breaking in tension was reported.⁵ Based on the measured force required to break the nanotube, a tensile strength of 150 GPa (experimental uncertainty $\sim 30\%$) at a deformation estimated to be $\sim 5\%$ was reported.

* Corresponding author.

[†] International Technology Center.

[‡] North Carolina State University.

[§] Northwestern University.

Table 2: Nanometer-Scale Mechanical Properties of Diamond and Graphite^a

structure	orientation	ab initio tensile fracture force per atom ^b (nN)	surface area per atom at the fracture plane S_{\perp} (\AA^2)	second derivative of strain energy (eV/atom) ^c	critical diameters for diamond rods (nm)	$Y_b S_{\perp}$ (nN)
diamond	$\langle 001 \rangle$	14.3	6.35	37.2	1.28	66.7
	$\langle 011 \rangle$	5.85	4.45	41.3	2.17	51.8
	$\langle 111 \rangle$	5.2	5.47	42.8	3.0	66.0
graphene	armchair	14.9	6.6	59		
	zigzag	17.5	8.36	57.3		85.3
SWNTs				~ 56		

^a Predicted critical diameters for DNRs correspond to the values above which DNRs become stronger than SWNTs of the corresponding diameter. ^b From ref 9 (diamond) and ref 4 (graphene). ^c Estimates based on the experimental Young's modulus for diamond (Table 1) and using ab initio data in ref 3 for graphene and SWNTs.

Although the overall load bearing properties of MWNTs are impressive, it is important to note that there are limitations for exploiting this property for practical applications. For example, experiments by Yu et al. have shown that when clamps are applied to the outermost shell of a MWNT and the MWNT is tensile loaded, failure occurs only in the outermost shell.⁶ This result suggests very limited load transfer between the outer and inner shells, and therefore the inner shells under these conditions apparently do not significantly contribute to the load bearing cross sectional area of the system.

The measured and predicted Young's moduli of bulk diamond are similar to that of carbon nanotubes, especially in the $\langle 111 \rangle$ direction (Table 1). The strength measured at the edge of contact of a Hertzian indenter and a diamond flat is 60 GPa.⁷ The predicted ultimate strength of diamond, which exhibits almost ideal cleavage, is about 100 and 200 GPa in the $\langle 111 \rangle$ and $\langle 001 \rangle$ directions, respectively.^{8,9} These extreme macroscale mechanical properties suggest that if stable structures could be synthesized, DNRs would have mechanical properties that meet or exceed those of fullerene nanotubes.

Stress-strain relations are explicitly macroscopic scale properties that require a definition of cross sectional area. In the case of fullerene nanotubes, values of mechanical properties such as those above are typically derived assuming an effective cross sectional width of a carbon sheet that corresponds to the interplanar spacing of graphite (about 3.35 \AA).³ At the nanoscale, a less ambiguous characteristic of strength (at least for comparison of fiber-like nanostructures with similar diameters) is the maximum force before fracture for a given structure, rather than the maximum stress. Plotted in Figure 1 is the theoretical dependence of fracture force versus diameter for SWNTs, MWNTs, and DNRs. This analysis is based on forces for bond breaking between individual atoms (Table 2) and the number of atomic sites in the cross-sectional area of the nanostructures. For the nanotubes, we assume a $(n,0)$ structure and use the ideal strength value for a graphene sheet from ab initio pseudo-potential total energy calculations carried out within the local density approximation⁴ (the values are summarized in Tables 1 and 2). The MWNTs are assumed to have a fixed inner diameter of 4 nm, which is typical for these structures, and different numbers of outer shells assuming an inter-shell distance of 3.4 \AA . Three orientations for the DNRs are

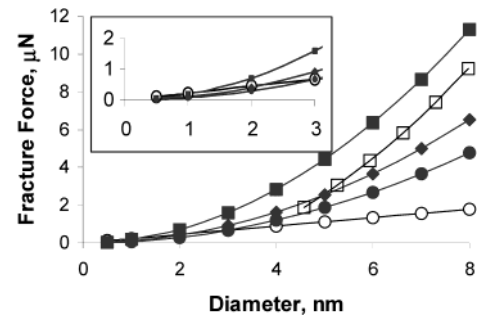


Figure 1. Predicted fracture force as a function of diameter.¹⁰ \circ SWNTs, \square MWNTs, \bullet $\langle 111 \rangle$ DNRs, \blacklozenge $\langle 011 \rangle$ DNRs, \blacksquare $\langle 001 \rangle$ DNRs. The diameter of the inner shell for all of the MWNTs is assumed to be 4 nm. Inset: Expanded view of the small diameter region of the results.

considered that have their long axis corresponding to one of three low-index axes, $\langle 111 \rangle$, $\langle 110 \rangle$, or $\langle 100 \rangle$. The strength values for different diamond orientations were obtained from first principles calculations carried out either by the same authors⁸ or by similar techniques.⁹ Therefore, all of the parameters for our evaluations are consistent with one another.

The results of Figure 1 suggest that at small diameters, SWNTs are stronger than DNRs because of the superior strength of single bonds in graphene over those in diamond (Table 2). However, as the diameter increases, the load bearing area (and correspondingly the total number of bonding sites) increases linearly for SWNTs and as the square of the diameter for DNRs, leading to a larger fracture force for DNRs above a critical diameter that is between 1 and 3 nm, depending on the orientation of the DNR (Table 2).

Two additional important factors to consider when comparing the mechanical properties of SWNTs and DNRs are their relative compactness and strength-to-weight ratio. From Figure 2 it is clear that DNRs are more compact than SWNTs, and therefore a DNR would in general displace less volume in a nanocomposite than a comparable SWNT. To illustrate the relative strength-to-weight ratios of DNRs and SWNTs, the ratio between the diameter of a DNR and a SWNT as a function of nanotube diameter is calculated for two cases, at the condition of equal fracture force and the condition of equal weight of the two structures being compared. At the equal fracture force condition for the two structures the DNR/SWNT weight ratio is constant and

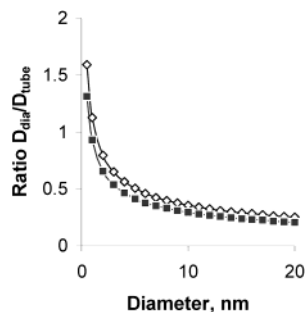


Figure 2. The ratio of the diameter of a DNR to a SWNT as a function of nanotube diameter at the conditions of equal fracture force (open diamonds) and equal weight of the structures (solid squares).

equals 1.47.¹¹ How diameters are related is apparent from Figure 2; at diameters smaller than the critical diameter, DNRs require a larger diameter to bear the same load as a related SWNT. At the requirement of equal weight, the ratio between the related fracture forces of DNR/SWNT is 0.68.¹² At larger diameters DNRs are therefore stronger but at the cost of a lower strength-to-weight ratio.

Similar to the strength analysis above, the stiffness of DNRs and SWNTs can be compared by considering them as nanoscale structures (rather than as materials). The thickness of the shells of carbon nanotubes required for estimating Young's modulus Y is an ambiguous parameter, but the product of Y and A (the cross-sectional area) is not because $Y \cdot A$ is directly proportional to the spring constant of the nanostructure. Rather than developing a stress-strain relationship, the dependence of elongation on applied force for SWNTs and DNRs with similar diameters is considered. To perform such an analysis, Hooke's law is used in terms attributed to individual atoms. A typical stress-strain relationship for uniform tension of a homogeneous system can be written as

$$F_a = S_{\perp} Y e \quad (1)$$

where F_a is the external load attributed to an atom, Y is the Young's modulus for a given orientation, e is the resulting deformation, and S_{\perp} is the area per atom in the cross-sectional area perpendicular to the direction of the applied force.

The Young's modulus of a bulk structure can be calculated using the volume per atom V_o and the second derivative of a strain energy $\partial^2 E / \partial \epsilon^2$ per atom, the latter providing an unambiguous characteristic of the elastic properties of nanoscale structures.¹³ Alternatively, the volume per atom can be described through other geometrical parameters of the structure as

$$Y = \frac{1}{V_o} \left(\frac{\partial^2 E}{\partial \epsilon^2} \right)_{\epsilon=0} = \frac{1}{S_{\parallel} h} \left(\frac{\partial^2 E}{\partial \epsilon^2} \right)_{\epsilon=0} = \frac{1}{S_{\perp} l} \left(\frac{\partial^2 E}{\partial \epsilon^2} \right)_{\epsilon=0} \quad (2)$$

Typically, the Young's modulus of a nanotube is calculated using the surface area per atom S_{\parallel} and the wall thickness of a nanotube h (usually assumed 0.335 nm in accordance with

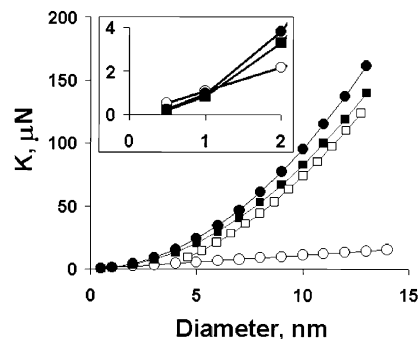


Figure 3. Plot of stiffness (eq 3) as a function of diameter of the nanostructure. Symbols are the same as Figure 1. Inset: Enlarged view of the small-diameter region of the plot.

the interlayer separation in graphite). The volume per atom can also be ascribed through the area per atom in the cross-sectional area perpendicular to the direction of the applied force S_{\perp} and a characteristic length per atom l along the direction of the applied force (the last expression in eq 2). Substituting the last expression in eq 2 into eq 1, it follows that the parameter $Y S_{\perp}$ is unambiguous, and can be calculated as a second derivative of strain energy divided by length attributed to an atom along the direction of the tensile force. This characteristic is significantly higher for graphite as compared to diamond (Table 2). This result reflects the fact that C-C bonds in graphite are substantially stiffer than those in diamond, but that the bulk materials have comparable stiffness (in-plane for graphite versus any direction in diamond) because of the higher density of diamond, 3.5 versus 2.2 g/cm³ for graphite.

For a nanostructure under tension and using eq 1, the relation for total force-strain is

$$f = F_a M = S_{\perp} Y M e = K e \quad (3)$$

where M is the number of atoms within a cross-sectional area for a nanotube/nanorod of a given diameter.^{11,12} A nanostructure stiffness K is introduced as a coefficient of proportionality between the applied force and elongation. It is a quantity, calculated using unambiguous parameters,¹⁵ that depends on the diameter of the nanorod (nanotube).¹⁴ The stiffness K as a function of diameter is illustrated in Figure 3 for DNRs, and for SWNTs and MWNTs. For a fixed diameter, K multiplied by elongation is the total force required to achieve the elongation. As can be seen from Figure 3, both $\langle 001 \rangle$ and $\langle 111 \rangle$ DNRs are stiffer than SWNTs at diameters exceeding ~ 1 nm.

The results above establish that DNRs are *important* target structures for synthesis. To explore whether DNRs are *viable* target structures, we have used molecular modeling to characterize binding energies for several example DNR structures. Illustrated in Figure 4 are four examples of modeled DNRs that have different crystal orientations along their long axis and different surface structures. These are high-symmetry structures with faces cut from low Miller index planes and therefore likely represent a subset of the most stable nanometer-scale structures of this type. It had

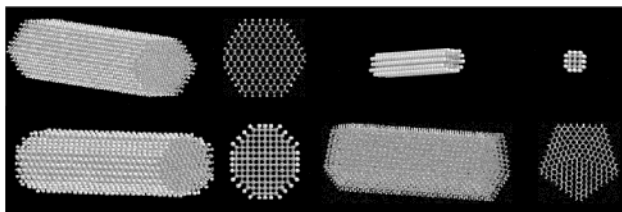


Figure 4. Ball-and-stick illustrations of representative DNRs. Upper left: Principal axis corresponds to the diamond $\langle 011 \rangle$ direction. Lower left: Principal axis corresponds to the $\langle 001 \rangle$ direction with (011) and (001) facets. Upper right: Principal axis corresponds to the diamond $\langle 001 \rangle$ direction, with (001) facets. Lower right: A twinned structure with principal axis corresponding to the diamond $\langle 011 \rangle$ direction and (001) facets.

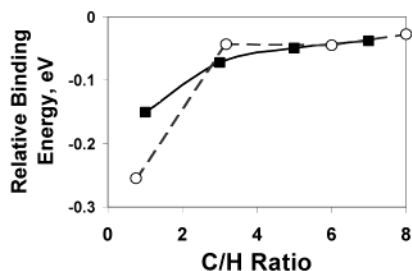


Figure 5. Binding energies given by a bond-order potential as a function of hydrogen-to-carbon ratio. Energies were calculated using a dimer reconstruction for all surfaces with structures corresponding to the (100) diamond surface. Open circles: diamond nanorods. Solid squares: (17,0) nanotubes of different lengths whose ends are hydrogen terminated. Energies are relative to systems of diamond and H_2 with the same C/H ratio.

been shown for diamond clusters that morphology (type and number of exposed faces) plays a significant role in their stability for both hydrogenated (most stable) and bare surfaces.¹⁴ Plotted in Figure 5 are energies as a function of the carbon-to-hydrogen ratio for the four diamond nanorods illustrated in Figure 4. To compare these energies to equivalent SWNTs, also plotted in Figure 5 are energies for (17,0) SWNTs of finite length whose ends have been hydrogen terminated. The energies reported were calculated using a many-body bond-order potential¹⁶ and are relative to systems with the same number of carbon and hydrogen atoms in graphite and as H_2 molecules, respectively. For large carbon-to-hydrogen ratios, the DNRs and the SWNTs are roughly comparable in binding energy, while for small ratios the sp^3 -bonded structures are energetically favored, in agreement with a previous analysis of carbon-hydrogen clusters.¹⁷

The results of the modeling reported here suggest that DNRs are desirable for their mechanical properties and are energetically competitive with SWNTs, especially for small hydrogen-to-carbon ratios. Given the number of methods that have been used to produce covalently bonded inorganic whiskers, the prospects for synthesizing DNRs appear very promising. For example, β -SiC whiskers with radii as small as 10 nm have been synthesized by a number of methods, including hot filament chemical vapor deposition,¹⁸ laser ablation,¹⁹ reduction-carburization,²⁰ and sol-gel reactions followed by carbothermal reduction of xerogels.²¹ Aligned

diamond whiskers have been formed by air plasma etching of polycrystalline diamond films, particularly as-grown diamond films,²² where nanowhiskers were found to form preferentially at grain boundaries of diamond crystals and in films with molybdenum deposited as an etch-resistant mask.^{22,23} By dry etching diamond films with preformed Mo deposits that acted as etch stops that protect the diamond beneath small Mo islands, well-aligned diamond nanorods 60 nm in diameter were formed that had a density of 50 μm^2 over the entire film surface.²² The synthesis of well-aligned diamond cylinders in an anodic aluminum oxide template using microwave plasma-assisted chemical vapor deposition was recently reported.²⁴ The cylinders had lengths of about 5 μm and average diameters of about 300 nm.

Interestingly, fabrication by a variety of techniques of diamond rods with diameters as small as 10 μm and lengths of several hundred microns have been reported starting in the 1960s.^{25–27} The rods were grown epitaxially from the gas phase under low-pressure conditions on diamond seed crystals wetted with Ni, Fe, or Mn.²⁵ The growth of single-crystal diamond filaments was also reported.²⁵ Diamond whiskers were also grown in an electron microscope on the sharp edges of diamond or other dielectric crystals under electron beam irradiation from carbon-containing residual gases at low pressures.²⁶ Diamond whisker growth in a metal-carbon system at high pressure and temperature conditions has also been reported.²⁷ Finally, a book²⁸ briefly mentions a study in which aggregates of needle-like diamond crystals and particles with sharp edges of about 10 nm in size were produced by a shock wave process, suggesting that diamond nanowhiskers could potentially be produced by detonation synthesis.

Acknowledgment. The authors are thankful to David Roundy and Frank Fisher for useful discussions. O.A.S. acknowledges support from the Office of Naval Research through contract N00014-95-1-0270. D.W.B. acknowledges support from the Office of Naval Research through contract N00014-95-1-0270 and through a subcontract from the University of North Carolina at Chapel Hill, and from NASA-Ames and NASA-Langley. R.S.R. acknowledges support from the NASA University Research, Engineering and Technology Institute on Bio Inspired Materials under award No. NCC-1-02037, and from the Office of Naval Research through contract N000140210870.

References

- (1) Yu, M. F.; Files, B. S.; Arepalli, S.; Ruoff, R. S. *Phys. Rev. Lett.* **2000**, *84*, 5552.
- (2) Buongiorno Nardelli, M.; Yakobson, B. I.; Bernholc, J. *Phys. Rev. B* **1998**, *57*, R4277.
- (3) Kudin, K. N.; Scuseria, G. E.; Yakobson, B. I. *Phys. Rev. B* **2001**, *64*, 235406.
- (4) Ribeiro, F. J.; Roundy, D. J.; Cohen, M. L. *Phys. Rev. B* **2002**, *65*, 153401.
- (5) Demczyk, B.; Wang, Y. M.; Cumings, J.; Hetman, M.; Han, W.; Zettl, A.; Ritchie, R. O. *Mater. Sci. Eng. A* **2002**, *334*, 173.
- (6) Yu, M. F.; Lourie, O.; Dyer, M. J.; Moloni, K.; Kelly, T. F.; Ruoff, R. S. *Science* **2000**, *287*, 637.
- (7) Field, J. E. *The Properties of Natural and Synthetic Diamond*; Academic: London, 1992.
- (8) Roundy, D.; Cohen, M. L. *Phys. Rev. B* **2001**, *64*, 212103.

- (9) Telling, R. H.; Pickard, C. J.; Payne, M. C.; Field, J. E. *Phys. Rev. Lett.* **2000**, *84*, 5160.
- (10) The fracture loads F versus diameter D for Figure 1 were calculated as follows. For DNRs, $F_{\text{dia}} = N_{\text{dia}} \times f_{\text{dia}} = \pi D^2 / (4S_o) \times f_{\text{dia}}$, where S_o is the area per atom in a cross section of a diamond rod and f_{dia} is the fracture force per atom for a nanorod with a particular orientation from Table 2. For SWNTs, $F_{\text{tube}} = N_{\text{tube}} \times f_{\text{tube}} = \pi D / (L_o) \times f_{\text{tube}}$, where L_o is an interatomic distance at the edges of a tube (0.246 nm for a zigzag nanotube) and f_{tube} is the fracture force per atom for a nanotube with a particular orientation from Table 2. For a MWNT, the analysis is the same as for a SWNT, but $N_{\text{tube}} = \pi(D_o(N+1) + 0.68N) / L_o$, where D_o is the inner diameter and N is the number of walls.
- (11) From the condition of equal fracture force (using equations from ref 10), we obtain the ratio r between the corresponding diameters for a SWNT and a DNR of the form $r = D_{\text{dia}} / D_{\text{tube}} = (1.27 / D_{\text{tube}})^{1/2}$. The numerical values for a $\langle 001 \rangle$ oriented DNR and a zigzag SWNT from Table 2 have been substituted into formulas from ref 10 to produce the analysis of Figure 2. Because D_{dia} and D_{tube} are known (for a given fracture force), the ratio between the number of atoms M_{tube} in a SWNT of length h and number of atoms M_{dia} in a DNR of the same length provides the weight ratio. In particular, $M_{\text{dia}} = \pi D_{\text{dia}}^2 h / 4V_o$, where V_o is the atomic volume of diamond atoms, and $M_{\text{tube}} = \pi D_{\text{tube}} h / S_t$, where S_t is a surface area per atom on a SWNT surface (0.0262 nm²). From the above relation $M_{\text{dia}} / M_{\text{tube}} = 1.16 D_{\text{dia}}^2 / D_{\text{tube}} = 1.47$.
- (12) From the condition of equal weight ($M_{\text{dia}} = M_{\text{tube}}$), the relationship between the diameters of a SWNT and a DNR will be $D_{\text{dia}} = (D_{\text{tube}} / 1.16)^{1/2}$. Using this relation in the equations of ref 10 to estimate fracture forces, the ratio between fracture forces of a DNR and a SWNT corresponding to this condition will be $F_{\text{dia}} / F_{\text{tube}} = 0.68$ using the numerical values for a $\langle 001 \rangle$ DNR and a zigzag SWNT.
- (13) Robertson, D. H.; Brenner, D. W.; Mintmire, J. W. *Phys. Rev. B* **1992**, *45*, 12592.
- (14) Russo, S. P.; Barnard, A. S.; Snook, I. K. *Philos. Mag. Lett.* **2003**, *83*, 39.
- (15) The nanostructural stiffness (size-dependent) is $K_{\text{SWNT}} = h \times 2\pi R$; $Y_t = 2\pi R(1/S_t)((\partial^2 E / \partial \epsilon^2))_{\epsilon=0}$; $K_{\text{MWNT}} = h\pi(D_o(N+1) + 0.68M)Y_t$, where D_o is the inner diameter, and N is a number of walls. $K_{\text{rod}} = \pi R^2 Y_d = \pi R^2(1/l)((\partial^2 E / \partial \epsilon^2))_{\epsilon=0}$.
- (16) Brenner, D. W.; Shenderova, O. A.; Harrison, J. A.; Stuart, S. J.; Ni, B.; Sinnott, S. B. *J. Phys.: Solid State* **2002**, *14*, 783.
- (17) Badziag, P.; Verwoerd, W. S.; Ellis, W. P.; Greiner, N. R. *Nature* **1990**, *343*, 244.
- (18) Peng, H. Y.; Zhou, X. T.; Lai, H. L.; Wang, N.; Lee, S. T. *J. Mater. Res.* **2000**, *15*, 2020.
- (19) Shi, W. S.; Zheng, Y. F.; Peng, H. Y.; Wang, N.; Lee, C. S.; Lee, S. T. *J. Am. Ceram. Soc.* **2000**, *83*, 3228.
- (20) Hu, J. Q.; Lu, Q. K.; Tang, K. B.; Deng, B.; Jiang, R. R.; Qian, Y. T.; Yu, W. C.; Zhou, G. E.; Liu, X. M.; Wu, J. X. *J. Phys. Chem. B* **2000**, *104*, 5251.
- (21) Meng, G. W.; Cui, Z.; Zhang, L. D.; Phillipp, F. *J. Cryst. Growth* **2000**, *209*, 801.
- (22) Baik, E.-S.; Baik, Y.-J.; Jeon, D. *J. Mater. Res.* **2000**, *15*, 923.
- (23) Baik, E.-S.; Baik, Y.-J.; Lee, S. W.; Jeon, D. *Thin Solid Films* **2000**, *377/378*, 295.
- (24) Masuda, H.; Yanagishita, T.; Yasui, K.; Nishio, K.; Yagi, I.; Rao, T. N.; Fijishima, A. *Adv. Mater.* **2001**, *13*, 247.
- (25) Deryagin, B. V.; Fedoseev, D. V.; Luk'yanovich, V. M.; Spitsin, B. V.; Ryabov, V. A.; Lavrent'ev, A. V. *J. Cryst. Growth* **1968**, *2*, 380.
- (26) Zamozhskii, V. D.; Luzin, A. N. *Dokl. Akad. Nauk SSSR* **1975**, *224*, 369 (in Russian).
- (27) Butuzov, V. P.; Laptev, V. A.; Dunin, V. P.; Zadneprovskii, B. I.; Sanzharlinskii, N. G. *Dokl. Akad. Nauk SSSR* **1975**, *225*, 88, (in Russian).
- (28) Vereschagin, A. L. *Detonation Nanodiamonds*; Altai State Technical University: Barnaul, Russian Federation, 200 (in Russian). Pierson, H. O. *Handbook of Carbon, Graphite, Diamond, and Fullerenes: Properties, Processing and Applications*; Noyes Publications: Park Ridge, NJ, 1993.

NL025949T